

## Blue and Near-UV Phosphorescence from Iridium Complexes with Cyclometalated Pyrazolyl or *N*-Heterocyclic Carbene Ligands

Tissa Sajoto, Peter I. Djurovich, Arnold Tamayo, Muhammed Yousufuddin, Robert Bau, and Mark E. Thompson\*

Department of Chemistry, University of Southern California, Los Angeles, California 90089-0744

Russell J. Holmes and Stephen R. Forrest\*

Department of Electrical Engineering, Princeton University, Princeton, New Jersey 08544

Received August 1, 2005

Two approaches are reported to achieve efficient blue to near-UV emission from triscyclometalated iridium(III) materials related to the previously reported complex, *fac*-Ir(ppz)<sub>3</sub> (ppz = 1-phenylpyrazolyl-*N,C*<sup>2'</sup>). The first involves replacement of the phenyl group of the ppz ligand with a 9,9-dimethyl-2-fluorenyl group, i.e., *fac*-tris(1-[(9,9-dimethyl-2-fluorenyl)]pyrazolyl-*N,C*<sup>2'</sup>)iridium(III), abbreviated as *fac*-Ir(flz)<sub>3</sub>. Crystallographic analysis reveals that both *fac*-Ir(flz)<sub>3</sub> and *fac*-Ir(ppz)<sub>3</sub> have a similar coordination environment around the Ir center. The absorption and emission spectra of *fac*-Ir(flz)<sub>3</sub> are red shifted from those of *fac*-Ir(ppz)<sub>3</sub>. The *fac*-Ir(flz)<sub>3</sub> complex gives blue photoluminescence (PL) with a high efficiency ( $\lambda_{\text{max}} = 480 \text{ nm}$ ,  $\phi_{\text{PL}} = 0.38$ ) at room temperature. The lifetime and quantum efficiency were used to determine the radiative and nonradiative rates ( $1.0 \times 10^4$  and  $2.0 \times 10^4 \text{ s}^{-1}$ , respectively). The second approach utilizes *N*-heterocyclic carbene (NHC) ligands to form triscyclometalated Ir complexes. Complexes with two different NHC ligands, i.e., iridium tris(1-phenyl-3-methylimidazolin-2-ylidene-*C,C*<sup>2'</sup>), abbreviated as Ir(pmi)<sub>3</sub>, and iridium tris(1-phenyl-3-methylbenzimidazolin-2-ylidene-*C,C*<sup>2'</sup>), abbreviated as Ir(pmb)<sub>3</sub>, were both isolated as facial and meridional isomers. Comparison of the crystallographic structures of the *fac*- and *mer*-isomers of Ir(pmb)<sub>3</sub> with the corresponding Ir(ppz)<sub>3</sub> isomers indicates that the imidazolyl-carbene ligand has a stronger trans influence than pyrazolyl and, thus, imparts a greater ligand field strength. Both *fac*-Ir(pmi)<sub>3</sub> and *fac*-Ir(pmb)<sub>3</sub> complexes display strong metal-to-ligand-charge-transfer absorption transitions in the UV ( $\lambda = 270\text{--}350 \text{ nm}$ ) and phosphoresce in the near-UV region ( $E_{0-0} = 380 \text{ nm}$ ) at room temperature with  $\phi_{\text{PL}}$  values of 0.02 and 0.04, respectively. The radiative decay rates for *fac*-Ir(pmi)<sub>3</sub> and *fac*-Ir(pmb)<sub>3</sub> ( $5 \times 10^4 \text{ s}^{-1}$  and  $18 \times 10^4 \text{ s}^{-1}$ , respectively) are somewhat higher than that of *fac*-Ir(flz)<sub>3</sub>, but the nonradiative rates are two orders of magnitude faster (i.e.,  $(2\text{--}4) \times 10^6 \text{ s}^{-1}$ ).

### Introduction

Luminescent Ir(III) complexes have exhibited enormous potential in a range of photonic applications. For example, these Ir complexes can be used as emissive dopants in organic light emitting devices (OLEDs),<sup>1,2</sup> sensitizers for

outer-sphere electron-transfer reactions,<sup>3,4</sup> photocatalysts for CO<sub>2</sub> reduction,<sup>5</sup> photoreductants<sup>6</sup> and singlet oxygen sensitizers,<sup>7</sup> as well as biological labeling reagents.<sup>8</sup> In particular, cyclometalated iridium complexes with emission colors that vary from blue to red have received a great deal of attention recently for their application to light emitting diodes.<sup>2,9</sup> Since the optical properties and related uses of the cyclometalated Ir complexes are strongly dependent on the characteristics of their ground and lowest excited states, it has become desirable to better understand the interactions between these states and thus determine how to systematically alter the photophysical properties by appropriate ligand or complex

\* To whom correspondence should be addressed. E-mail: met@usc.edu (M.E.T.), forrest@princeton.edu (S.R.F.).

(1) (a) Baldo, M. A.; O' Brien, D. F.; You, Y.; Shoustikov, A.; Sibley, S.; Thompson, M. E.; Forrest, S. R. *Nature* **1998**, *395*, 151. (b) Baldo, M. A.; Lamansky, S.; Burrows, P. E.; Thompson, M. E.; Forrest, S. R. *Appl. Phys. Lett.* **1999**, *75*, 4. (c) Thompson, M. E.; Burrows, P. E.; Forrest, S. R. *Curr. Opin. Solid State Mater. Sci.* **1999**, *4*, 369. (d) Baldo, M. A.; Thompson, M. E.; Forrest, S. R. *Nature* **2000**, *403*, 750.

design. Moreover, the formation of a high energy emitting species would be beneficial for many of the proposed applications for these materials. To these ends, we report a study of the synthesis and photophysical properties of cyclometalated Ir complexes, some of which emit in the near-UV part of the spectrum, with *N*-pyrazolyl- or imidazolyl-type carbene ligands.

The emission energies of luminescent cyclometalated Ir complexes are principally determined by the triplet energy of the cyclometalating ligand (C $\wedge$ N). To understand the strategies used to alter the emission energies by C $\wedge$ N ligand modification, the *fac*-Ir(ppy)<sub>3</sub> complex (ppy = 2-phenylpyridyl, Figure 1) can be used as a prototypical cyclometalated phosphor.<sup>6</sup> Both ligand- and metal-based orbitals are involved in the excited states of this complex. The phenyl group of ppy carries a formal negative charge; the highest occupied molecular orbital (HOMO) is principally composed of  $\pi$  orbitals of the phenyl ring and the metal d orbitals. The pyridine is formally neutral and the principal contributor to the lowest unoccupied molecular orbital (LUMO). The absorption spectra of the complex display strong metal-to-ligand-charge-transfer (MLCT) transitions at energies lower than the ligand  $\pi$ - $\pi^*$  transitions. The MLCT absorption bands have been assigned to transitions between the metal-ligand HOMO and ligand-localized LUMO orbitals.<sup>10</sup> However, the low temperature emission spectrum resembles simple ligand phosphorescence, suggesting decay from a ligand-localized (<sup>3</sup>LC,  $\pi$ - $\pi^*$ ) lowest excited state.<sup>11</sup> The radiative lifetime for the complex is ca. 2  $\mu$ s at room

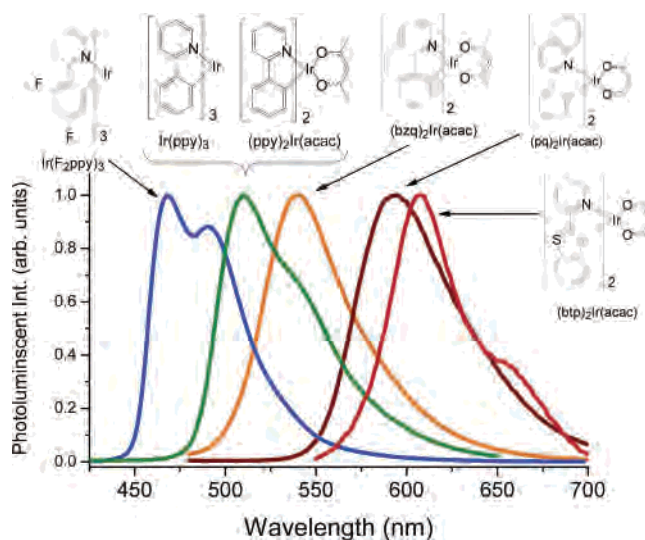


**Figure 1.** Photoluminescence spectra of Ir phosphors (room temperature, 2-MeTHF solutions).

temperature, which is indicative of a strong perturbation of the <sup>3</sup>LC state by participation of the singlet MLCT state through spin-orbit coupling. Thus, the lowest excited state of the complex is best described as an admixture of <sup>3</sup>LC and singlet metal-to-ligand-charge-transfer (<sup>1</sup>MLCT) states.<sup>12</sup>

The Ir complexes with ppy ligands emit green light,  $\lambda_{\text{max}} = 515$  nm, for both *fac*-Ir(ppy)<sub>3</sub> and (ppy)<sub>2</sub>Ir(acac) (acac = 2,4-pentanedionato-*O,O*, Figure 1). If the C $\wedge$ N  $\pi$ -system of the phenyl and pyridyl ligands is expanded by a bridging vinyl group, i.e., (bzq)<sub>2</sub>Ir(acac), a bathochromic shift is observed. If the  $\pi$ -system of the pyridyl fragment is enlarged using a 2-quinolyl moiety, e.g., (pq)<sub>2</sub>Ir(acac) in Figure 1, the emission color red shifts further.<sup>2h</sup> A similar red shift occurs when the phenyl fragment of ppy is replaced with a benzothiophene group ((btp)<sub>2</sub>Ir(acac), Figure 1). On the other hand, attempts to blue shift the emission spectrum by decreasing the size of the C $\wedge$ N  $\pi$ -system, e.g., replacing the phenyl ring with a vinyl group, also lead to a red shifted emission.<sup>13</sup> The decrease in emission energy in this case is understandable when one considers that the electron-electron repulsion in the triplet state increases with reduction in the size of the  $\pi$ -system, thereby lowering the triplet energy through increased singlet-triplet splitting (greater exchange energy).<sup>14</sup> For example, the triplet energies of vinyl substituted benzene derivatives are ca. 5 kcal mol<sup>-1</sup> (0.2 eV)<sup>15</sup> lower than that of biphenyl ( $E_{0-0} = 436$  nm, 2.84 eV).<sup>16</sup>

- (2) (a) Lamansky, S.; Djurovich, P. I.; Abdel-Razzaq, F.; Garon, S.; Murphy, D. L.; Thompson, M. E. *J. Appl. Phys.* **2002**, *92*, 1570. (b) Chen, F. C.; Yang, Y.; Thompson, M. E.; Kido, J. *Appl. Phys. Lett.* **2002**, *80*, 2308. (c) Markham, J. P. J.; Lo, S.-C.; Magennis, S. W.; Burn, P. L.; Samuel, I. D. W. *Appl. Phys. Lett.* **2002**, *80*, 2645. (d) Zhu, W.; Mo, Y.; Yuan, M.; Yang, W.; Cao, Y. *Appl. Phys. Lett.* **2002**, *80*, 2045. (e) Adachi, C.; Baldo, M. A.; Forrest, S. R.; Thompson, M. E. *J. Appl. Phys.* **2001**, *90*, 4058. (f) Ikai, M.; Tokito, S.; Sakamoto, Y.; Suzuki, T.; Taga, Y. *Appl. Phys. Lett.* **2001**, *79*, 156. (g) Adachi, C.; Lamansky, S.; Baldo, M. A.; Kwong, R. C.; Thompson, M. E.; Forrest, S. R. *Appl. Phys. Lett.* **2001**, *78*, 1622. (h) Lamansky, S.; Djurovich, P. I.; Murphy, D.; Abdel-Razzaq, F.; Lee, H. E.; Adachi, C.; Burrows, P. E.; Forrest, S. R.; Thompson, M. E. *J. Am. Chem. Soc.* **2001**, *123*, 4304.
- (3) (a) Sutin, N. *Acc. Chem. Res.* **1968**, *1*, 225. (b) Meyer, T. J. *Acc. Chem. Res.* **1978**, *11*, 94.
- (4) Schmid, B.; Garces, F. O.; Watts, R. J. *Inorg. Chem.* **1994**, *33*, 9.
- (5) (a) Belmore, K. A.; Vanderpool, R. A.; Tsai, J. C.; Khan, M. A.; Nicholas, K. M. *J. Am. Chem. Soc.* **1988**, *110*, 2004. (b) Silavwe, N. D.; Goldman, A. S.; Ritter, R.; Tyler, D. R. *Inorg. Chem.* **1989**, *28*, 1231.
- (6) King, K. A.; Spellane, P. J.; Watts, R. J. *J. Am. Chem. Soc.* **1985**, *107*, 1431.
- (7) (a) Demas, J. N.; Harris, E. W.; McBride, R. P. *J. Am. Chem. Soc.* **1977**, *99*, 3547. (b) Demas, J. N.; Harris, E. W.; Flynn, C. M.; Diemente, J. D. *J. Am. Chem. Soc.* **1975**, *97*, 3838. (c) Gao, R.; Ho, D. G.; Hernandez, B.; Selke, M.; Murphy, D.; Djurovich, P. I.; Thompson, M. E. *J. Am. Chem. Soc.* **2002**, *124*, 14828.
- (8) Lo, K. K.-W.; Chung, C.-K.; Lee, T. K.-M.; Lui, L.-K.; Tsang, K. H.-K.; Zhu, N. *Inorg. Chem.* **2003**, *42*, 6886.
- (9) (a) Li, J.; Djurovich, P. I.; Alleyne, B. D.; Tsyba, I.; Ho, N. N.; Bau, R.; Thompson, M. E. *Polyhedron* **2004**, *23*, 419. (b) Holmes, R. J.; Forrest, S. R.; Tung, Y. J.; Kwong, R. C.; Brown, J. J.; Garon, S.; Thompson, M. E. *Appl. Phys. Lett.* **2003**, *82*, 2422. (c) Holmes, R. J.; D'Andrade, B. W.; Forrest, S. R.; Ren, X.; Thompson, M. E. *Appl. Phys. Lett.* **2003**, *83*, 3818. (d) Ren, X.; Li, J.; Holmes, R. J.; Djurovich, P. I.; Forrest, S. R.; Thompson, M. E. *Chem. Mater.* **2004**, *16*, 4743.
- (10) (a) Stampor, W.; Mężyk, J.; Kalinowski, J. *Chem. Phys.* **2004**, *300*, 189–195. (b) Hay, P. J. *J. Phys. Chem. A* **2002**, *106*, 1634.
- (11) Finkelstein, W.; Yersin, H. *Chem. Phys. Lett.* **2004**, *300*.

- (12) (a) Colombo, M. G.; Güdel, H. *Inorg. Chem.* **1993**, *32*, 3081. (b) Strouse, G. F.; Güdel, H. U.; Bertolasi, V.; Ferretti, V. *Inorg. Chem.* **1995**, *34*, 5578. (c) Lever, A. P. B. *Inorganic Electronic Spectroscopy*, 2nd ed.; Elsevier: New York, 1984; p 174. (d) Wiedenhofer, H.; Schützenmeier, S.; von Zelewsky, A.; Yersin, H. *J. Phys. Chem.* **1995**, *99*, 13385. (e) Yersin, H.; Donges, D. *Top. Curr. Chem.* **2001**, *214*, 81–186. (f) Vanhelmont, F. W. M.; Güdel, H. U.; Förtsch, M.; Bürgi, H.-B. *Inorg. Chem.* **1997**, *36*, 5512.
- (13) Paulose, B. M. J. S.; Rayabharapu, D. K.; Duan, J.-P. Cheng, C.-H. *Adv. Mater.* **2004**, *16*, 2003.
- (14) Turro, N. J. *Modern Molecular Photochemistry*; Benjamin/Cummings: Menlo Park, 1978; pp 30–32.
- (15) (a) Ni, T.; Caldwell, R. A.; Melton, L. A. *J. Am. Chem. Soc.* **1989**, *111*, 457–464. (b) Ramamurthy, V.; Caspar, J. V.; Eaton, D. F.; Kuo, E. W.; Corbin, D. R. *J. Am. Chem. Soc.* **1992**, *114*, 3882–3892.
- (16) Taylor, H. V.; Allred, A. L.; Hoffman, B. M. *J. Am. Chem. Soc.* **1973**, *95*, 3215–3219.

Therefore, alternative methods are required to increase the triplet energies of Ir complexes with cyclometalated aromatic ligands.

A number of approaches to increase the emission energy of cyclometalated Ir complexes have focused on methods to decrease the HOMO energy while keeping the LUMO energy relatively unchanged. The addition of electron withdrawing groups to the phenyl ring has been used as one way to achieve this goal.<sup>17,18a</sup> The most common electron withdrawing group used for this purpose is fluoride, and a typical example of this blue shifting is seen for *fac*-Ir(F<sub>2</sub>ppy)<sub>3</sub> in Figure 1.<sup>18a</sup> An alternate approach to lower the HOMO energy involves the use of ancillary ligands to tune the HOMO energies of biscyclometalated derivatives. We have recently reported a detailed study of ancillary ligand effects on the emission energies of (C<sup>^</sup>N)<sub>2</sub>Ir(L<sup>^</sup>X) complexes.<sup>19</sup> The emission energy can be significantly increased by judicious choice of the ancillary ligand; however, increasing the emission energy of the ppy<sub>2</sub>Ir(L<sup>^</sup>X) complexes to generate a saturated blue color leads to a pronounced decrease in luminance efficiency. The decline in quantum efficiency is due to a significant decrease in the radiative rates, relative to the nonradiative rates, which comes about from an increased separation between the <sup>1</sup>MLCT and <sup>3</sup>LC energies as a result of the decreased HOMO energy.<sup>19</sup>

In contrast to methods which rely on altering the HOMO energy to blue shift the phosphorescence of cyclometalated Ir complexes, the strategy described herein involves replacing the heterocyclic fragment of the C<sup>^</sup>N ligands with moieties that destabilize the LUMO relative to that of a cyclometalated ppy ligand. We show that replacing the pyridyl ring with either an *N*-pyrazolyl or *N*-heterocyclic carbene-based group leads to a significant increase in the LUMO energy and, consequently, increases the emission energy of complexes coordinated to these ligands. It, thus, becomes possible to observe efficient blue or near-UV phosphorescence at room temperature from Ir complexes that have cyclometalated *N*-pyrazolyl- or carbene-based ligands.

## Results and Discussion

**Cyclometalated Pyrazolyl-Based Ligands for Blue Phosphorescence.** The effect that an increase in the LUMO energy has on tricyclic Ir complexes can be illustrated by comparing the electrochemical and photophysical properties of *fac*-Ir(ppy)<sub>3</sub> with those of the analogous complex that has a ligand with a high triplet energy, *fac*-Ir(ppz)<sub>3</sub> (ppz = 1-phenylpyrazolyl).<sup>18,20</sup> Both Ir complexes

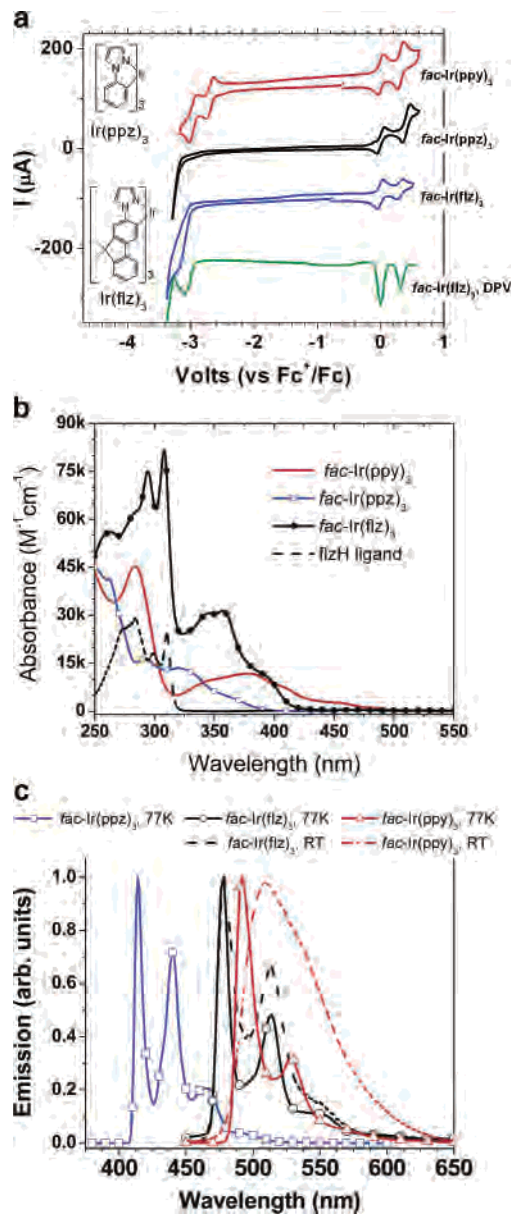


**Figure 2.** (a) Cyclic voltammograms (CV) traces, (b) absorption spectra, and (c) emission spectra for *fac*-Ir(ppy)<sub>3</sub>, *fac*-Ir(ppz)<sub>3</sub>, and *fac*-Ir(flz)<sub>3</sub>. The DPV trace for *fac*-Ir(flz)<sub>3</sub> is also shown. The wave at 0 V in each of the CV traces is the ferrocene reference; the *fac*-Ir(ppy)<sub>3</sub> and *fac*-Ir(flz)<sub>3</sub> traces are offset in the current axis for clarity. Absorption spectra were recorded at room temperature, and emission spectra were recorded in 2-MeTHF solutions at either 77 K or room temperature (see legend).

have similar HOMO energies; however, the LUMO energy of *fac*-Ir(ppz)<sub>3</sub> is shifted to a considerably higher energy relative to that of *fac*-Ir(ppy)<sub>3</sub>. This difference in electronic energy is reflected in the redox properties of the two species (Figure 2). The oxidation potentials for the two complexes are nearly identical (*fac*-Ir(ppz)<sub>3</sub>,  $E_{1/2}^{ox} = 0.41$  V; *fac*-Ir(ppy)<sub>3</sub>,  $E_{1/2}^{ox} = 0.31$  V), while the reduction potentials are markedly different; that is, reduction for *fac*-Ir(ppz)<sub>3</sub> is not observed prior to solvent reduction ( $-3.2$  V vs Fc<sup>+/0</sup>/Fc), whereas *fac*-Ir(ppy)<sub>3</sub> displays two reduction waves under the

- (17) (a) Grushin, V. V.; Herron, N.; LeCloux, D. D.; Marshall, W. J.; Petrov, V. A.; Wang, Y. *J. Chem. Soc., Chem. Commun.* **2001**, 1494–1495. (b) Coppo, P.; Plummer, E. A.; De Cola, L. *J. Chem. Soc., Chem. Commun.* **2004**, 1774–1775. (c) Dedeian, K.; Shi, J.; Nigel, S.; Forsythe, E.; Morton, D. *Inorg. Chem.* **2005**, *44*, 4445–4447.
- (18) (a) Tamayo, A.; Alleyne, B.; Djurovich, P. I.; Lamansky, S.; Tsyba, I.; Ho, N.; Bau, R.; Thompson, M. E. *J. Am. Chem. Soc.* **2003**, *125*, 7377. (b) Adamovich, V.; Brooks, J.; Tamayo, A.; Alexander, A. M.; Djurovich, P. I.; D'Andrade, B. W.; Adachi, C.; Forrest, S. R.; Thompson, M. E. *New J. Chem.* **2002**, *26*, 1171.
- (19) Li, J.; Djurovich, P. I.; Alleyne, B. D.; Yousufuddin, M.; Ho, N. N.; Thomas, J. C.; Peters, J. C.; Bau, R.; Thompson, M. E. *Inorg. Chem.* **2005**, *44*, 1713.

- (20) (a) Nam, E. J.; Kim, J. H.; Kim, B.; Kim, S. M.; Park, N. G. *Bull. Chem. Soc. Jpn.* **2004**, *77*, 751–755. (b) Choi, G. C.; Lee, J. E.; Park, N. G.; Kim, Y. S. *Mol. Cryst. Liq. Cryst.* **2004**, *424*, 173–185.



same conditions ( $E_{1/2}^{\text{red}} = -2.70, -3.00 \text{ V}$ ).<sup>18a</sup> The higher LUMO energy of *fac*-Ir(ppz)<sub>3</sub> relative to that of *fac*-Ir(ppy)<sub>3</sub> is also manifested in the photophysical properties of the complexes. The MLCT absorption transitions of *fac*-Ir(ppz)<sub>3</sub> ( $\lambda_{\text{max}} = 321 \text{ nm}$ , 3.86 eV) are much higher in energy than those of *fac*-Ir(ppy)<sub>3</sub> ( $\lambda_{\text{max}} = 377 \text{ nm}$ , 3.29 eV) (Figure 2).<sup>18a</sup> Likewise, the emission energy of *fac*-Ir(ppz)<sub>3</sub> ( $E_{0-0} = 414 \text{ nm}$ , 3.00 eV) is greater than that of *fac*-Ir(ppy)<sub>3</sub> ( $E_{0-0} = 494 \text{ nm}$ , 2.51 eV) (Figure 2). The photophysical properties of the Ir complexes are mirrored by those of the ligands themselves. The triplet energy of the ppzH ligand (380 nm, 3.26 eV)<sup>21</sup> is much higher than that of ppyH (430 nm, 2.88 eV).<sup>22</sup> Notably, whereas the photoluminescent (PL) efficiency of *fac*-Ir(ppy)<sub>3</sub> is quite high and invariant with temperature (when dispersed in a solid matrix),<sup>23</sup> the PL efficiency of *fac*-Ir(ppz)<sub>3</sub> is strongly temperature dependent. No detectable emission from *fac*-Ir(ppz)<sub>3</sub> is observed in fluid or solid solutions at room temperature.<sup>24</sup> Weak emission from *fac*-Ir(ppz)<sub>3</sub> is only observed in fluid solutions at low temperature (<230 K), while intense emission occurs at 77 K. Evidently, *fac*-Ir(ppz)<sub>3</sub> decays nonradiatively by thermal population of a higher lying nonemissive excited state at room temperature.

Considerable work has been done to understand the thermally activated decay processes in luminescent transition metal complexes.<sup>25</sup> In particular, Ru(II) and Os(II) tris-diimines have been extensively studied in this regard, since the photophysical properties of these materials exhibit strong temperature-dependent behavior. It has been found that the temperature-dependent luminescence in Ru(II) diimine complexes is characteristic of thermal population to ligand field (dissociative) states, whereas the Os(II) analogues have kinetic parameters more consistent with deactivation through higher energy MLCT states.<sup>26</sup> The difference between the Os and Ru complexes is due to the larger ligand field splitting observed for 5d over 4d elements, which destabilizes the ligand field states in the Os analogues to energies that are thermally inaccessible from the emissive triplet. The cyclometalated Ir(III) complexes reported here are isoelec-

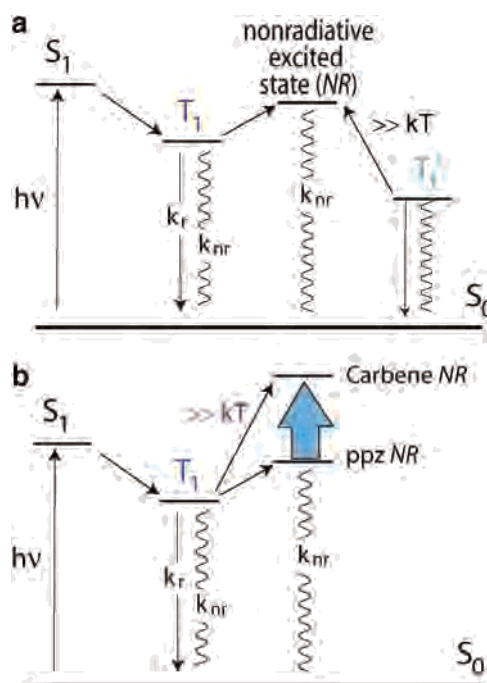


**Figure 3.** (a) Energy level scheme for emissions from *fac*-Ir(ppz)<sub>3</sub> ( $T_1$ ) and *fac*-Ir(flz)<sub>3</sub> ( $T_1$ ). The two compounds are expected to have nonradiative excited states (NR) with similar energies. (b) Energy level scheme for emissions from *fac*-Ir(ppz)<sub>3</sub> and *fac*-Ir(C<sup>∧</sup>C)<sub>3</sub> compounds.

tronic with the Ru(II) and Os(II) tris-diimine materials and are expected to mimic the photophysics of their Os(II) counterparts.<sup>27</sup> Thus, the *fac*-Ir(ppz)<sub>3</sub> complex could decay nonradiatively through higher energy MLCT states.<sup>20b</sup> However, the triplet energy of *fac*-Ir(ppz)<sub>3</sub> is very high (3.0 eV, 70 kcal mol<sup>-1</sup>) and comparable to the Ir-phenyl bond strength.<sup>28</sup> Therefore, thermal population to accessible ligand field states can also be considered to be a possible non-radiative luminescent decay mechanism. Another possible decay process could be through a ligand localized,  $n-\pi^*$  state. A schematic representation of the emission and potential thermally activated nonradiative decay processes of cyclometalated Ir complexes is given in Figure 3a. The absence of luminescence at room temperature requires that the rate of non-radiative decay ( $k_{\text{nr}}$ ) from the nonemissive excited state (NR state in Figure 3) be significantly greater than the radiative rate ( $k_r$ ). In addition, the energy difference between the emissive triplet ( $T_1$ ) and the NR states must be small enough that the higher energy nonemissive state is thermally accessible.

To achieve efficient luminescence from cyclometalated ppz-based Ir complexes at room temperature, it is necessary to retard or eliminate nonradiative processes that thermally deactivate the excited state. The pyrazolyl moiety itself is not the origin of emission decay, since several complexes with pyrazolyl-based ancillary ligands have very high PL efficiencies at room temperature.<sup>17c,29,30</sup> One way to suppress the luminescent deactivation in a complex is to lower the

(21) Pavlik, J. W.; Connors, R. E.; Burns, D. S.; Kurzwil, E. M. *J. Am. Chem. Soc.* **1993**, *115*, 7465.

(22) Maestri, M.; Sandrini, D.; Balzani, V.; Maeder, U.; von Zelewsky, A. *Inorg. Chem.* **1987**, *26*, 1323.

(23) Kawamura, Y.; Goushi, K.; Brooks, J.; Brown, J. J.; Sasabe, H.; Adachi, C. *Appl. Phys. Lett.* **2004**. Kawamura, Y.; Sasabe, H.; Adachi, C. *Jpn. J. Appl. Phys.* **2004**, *43*, 7729.

(24) The authors in ref 20a report a green emission at room temperature from solid state samples of *fac*-Ir(ppz)<sub>3</sub>. We have also observed a similar emission from neat solids of *fac*-Ir(ppz)<sub>3</sub> and attribute it to luminescence from an impurity in the material. Extensive purification of *fac*-Ir(ppz)<sub>3</sub> leads to weakly or nonemissive samples. Analysis of the green luminescence in the solid state by time-resolved spectroscopy shows that the emission displays a rise time of ca. 2  $\mu\text{s}$  at 77 K before decay. This temporal behavior is consistent with trap emission from an impurity in the solid. Moreover, the emission is only observed for neat solids. Samples of *fac*-Ir(ppz)<sub>3</sub> doped into polystyrene or other high triplet energy host materials are nonemissive at room temperature and show only the near-UV emission illustrated in Figure 2 at temperatures below 200 K.

(25) (a) Forster, L. S. *Coord. Chem. Rev.* **2002**, *227*, 59 and references therein. (b) Brennaman, M. K.; Meyer, T. J.; Papanikolas, J. M. *J. Phys. Chem. A* **2004**, *108*, 9938. (c) Wang, X.-Y.; Del Guerso, A.; Schmeil, R. H. *J. Photochem. Photobiol. C* **2004**, *5*, 55 and references therein.

(26) Lumpkin, R. S.; Kober, E. M.; Worl, L. A.; Murtaza, Z.; Meyer, T. J. *J. Phys. Chem.* **1990**, *94*, 239.

(27) Dixon, I. M.; Collin, J.-P.; Sauvage, J.-P.; Flamigni, L.; Encinas, S.; Barigelletti, F. *Chem. Soc. Rev.* **2000**, *6*, 385–391.

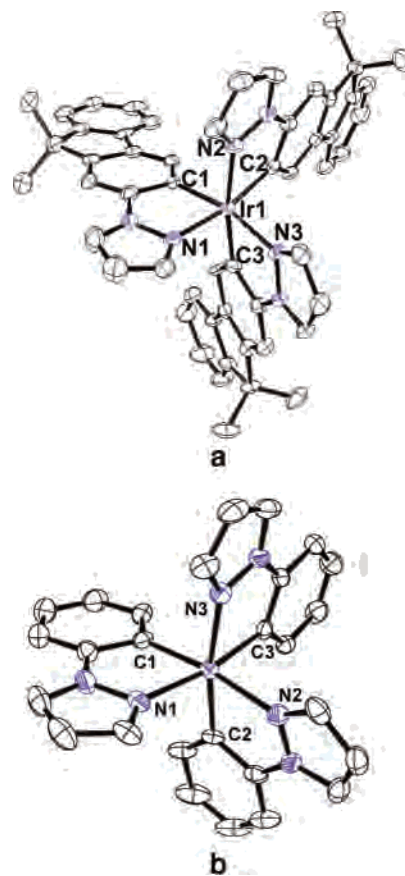
(28) Nolan, S. P.; Hoff, C. D.; Stoutland, P. O.; Newman, L. J.; Buchanan, J. M.; Bergman, R. G.; Yang, G. K.; Peters, K. S. *J. Am. Chem. Soc.* **1987**, *109*, 3143.

**Table 1.** Selected Bond Distances (Å) and Angles (deg) for *fac*- and *mer*-Ir(ppz)<sub>3</sub>,<sup>18a</sup> *fac*-Ir(flz)<sub>3</sub>, and *fac*- and *mer*-Ir(pmb)<sub>3</sub>

bond	Ir(ppz) <sub>3</sub> <sup>18a</sup>		Ir(flz) <sub>3</sub>		Ir(pmb) <sub>3</sub>	
	facial	meridional	facial	facial	meridional	meridional
Selected Bond Distances (Å)						
Ir1–N1	2.117(5)	2.053(2)	2.115(6)			
Ir1–N2	2.135(5)	2.026(2)	2.095(7)			
Ir1–N3	2.120(6)	2.013(2)	2.121(6)			
Ir1–C1	2.015(7)	2.051(2)	2.023(7)	2.077(7)	2.099(4)	
Ir1–C2	2.027(6)	2.057(2)	2.019(7)	2.071(7)	2.078(4)	
Ir1–C3	2.021(6)	1.993(2)	2.024(8)	2.094(7)	2.086(4)	
Ir1–C4				2.035(7)	2.043(4)	
Ir1–C5				2.022(7)	2.019(4)	
Ir1–C6				2.022(8)	2.032(4)	
Bond Angles (deg)						
N2–Ir1–N3	94.4(2)	171.54(8)	91.7(2)			
C1–Ir1–C2	93.7(3)	172.67(9)	92.2(3)	91.0(3)	90.91(16)	
C4–Ir1–C6				100.2(3)	93.96(16)	

energy of its triplet state to such a value that the NR state is no longer thermally accessible at room temperature. This concept was applied in the design of *fac*-Ir(flz)<sub>3</sub> (flz = 1-[(9,9-dimethyl-2-fluorenyl)]pyrazolyl), an analogue of *fac*-Ir(ppz)<sub>3</sub> in which the  $\pi$ -system of the ppz ligand is extended using a fluorenyl moiety. The incorporation of fluorenyl groups in cyclometalated Ir complexes has been previously reported and found to lower the triplet energy of Ir(ppy)<sub>3</sub> type derivatives.<sup>31</sup> In these earlier examples, however, the decreased triplet energy of the fluorenyl analogues had little impact on the luminescence efficiency of the complexes, since the *fac*-Ir(ppy)<sub>3</sub> complex is already highly emissive at room temperature.

The *fac*-Ir(flz)<sub>3</sub> complex was prepared by a two step procedure analogous to what we have reported for *fac*-Ir(ppz)<sub>3</sub>.<sup>18a</sup> Single crystals of *fac*-Ir(flz)<sub>3</sub> were analyzed by X-ray crystallography. The *fac*-Ir(flz)<sub>3</sub> complex is expected to have a similar electronic configuration around the iridium center as *fac*-Ir(ppz)<sub>3</sub>, and a comparison of metric parameters for both compounds supports a high degree of structural similarity between the two species. Selected bond lengths and bond angles of the two complexes are listed in Table 1, and molecular plots are shown in Figure 4. Both *fac*-Ir(flz)<sub>3</sub> and *fac*-Ir(ppz)<sub>3</sub> have a pseudo-octahedral coordination geometry of three pyrazolyl nitrogens and three phenyl

**Figure 4.** Thermal ellipsoid (ORTEP) plots of *fac*-Ir(flz)<sub>3</sub> (a) and *fac*-Ir(ppz)<sub>3</sub><sup>18a</sup> (b). The hydrogen atoms have been omitted for clarity. The atom numbering used in Table 1 is shown.

carbons in a facial arrangement. The Ir–N and Ir–C bond lengths for the two structures are statistically equivalent. The average Ir–N (2.110(6) Å) and Ir–C (2.022(7) Å) bond lengths of *fac*-Ir(flz)<sub>3</sub> are within one sigma of the corresponding averages for *fac*-Ir(ppz)<sub>3</sub> (average Ir–N = 2.124(5) Å, average Ir–C = 2.021(6) Å). The structural data suggest a nearly identical coordination environment around the Ir center for the two complexes, and thus, both are expected to have ligand field states with similar energies.

The influence of the extended  $\pi$ -system in *fac*-Ir(flz)<sub>3</sub> is apparent in the electrochemical properties of the complex. While the oxidation potential of *fac*-Ir(flz)<sub>3</sub> ( $E_{1/2}^{\text{ox}} = 0.31$  V) is similar to that of *fac*-Ir(ppz)<sub>3</sub>, a quasi-reversible reduction can now be discerned in the envelope of the solvent reduction wave (Figure 2). A distinct reduction process ( $E_{1/2}^{\text{red}} = -3.1$  V) can be identified using differential pulse voltammetric (DPV) analysis. The expanded aromatic ring system of *fac*-Ir(flz)<sub>3</sub> clearly serves to lower the LUMO energy of the complex.

The introduction of the fluorenyl chromophore has a marked impact on the absorption spectra of *fac*-Ir(flz)<sub>3</sub> (Figure 2). The complex displays a series of intense, high energy absorption bands ( $\lambda < 320$  nm,  $\epsilon > 5 \times 10^4$  M<sup>-1</sup> cm<sup>-1</sup>), which can be assigned to ligand localized  $\pi$ – $\pi^*$  transitions by comparison to the absorption spectrum of the flzH ligand (Figure 2). The extinction coefficients for these bands are roughly three times greater than those for the same

- (29) (a) Holmes, R. J.; D'Andrade, B. W.; Forrest, S. R.; Ren, X.; Thompson, M. E. *Appl. Phys. Lett.* **2003**, *83*, 3818. (b) Ren, X.; Li, J.; Holmes, R. J.; Djurovich, P. I.; Forrest, S. R.; Thompson, M. E. *Chem. Mater.* **2004**, *16*, 4743.
- (30) (a) Lo, K. K.; Chung, C.; Lee, T. K.; Lui, L.; Tsing, K. H.; Zhu, N. *Inorg. Chem.* **2003**, *42*, 6886. (b) Lo, K. K.; Chan, J. S.; Chung, C.; Lui, L. *Organometallics* **2004**, *23*, 3108. (c) Kwon, T.-H.; Cho, H. S.; Kim, M. K.; Kim, J.-W.; Kim, J.-J.; Lee, K. H.; Park, S. J.; Shin, I.-S.; Kim, H.; Shin, D. M.; Chung, Y. K.; Hong, J.-I. *Organometallics* **2005**, *24*, 1578–1585.
- (31) (a) Gong, X.; Robinson, M. R.; Ostrowski, J. C.; Moses, D.; Bazan, G. C.; Heeger, A. J. *Adv. Mater.* **2002**, *14*, 581. (b) Ostrowski, J. C.; Robinson, M. R.; Heeger, A. J.; Bazan, G. C. *Chem. Commun.* **2002**, 7, 784. (c) Gong, X.; Robinson, M. R.; Ostrowski, J. C.; Moses, D.; Bazan, G. C.; Heeger, A. J.; Liu, M. S.; Jen, A. K. *Adv. Mater.* **2003**, *15*, 45. (d) Gong, X.; Robinson, M. R.; Ostrowski, J. C.; Moses, D.; Bazan, G. C.; Heeger, A. J. *Appl. Phys. Lett.* **2005**, *86*, 171108. (e) Wu, F.; Su, H.; Shu, C.; Luo, L.; Diau, W.; Cheng, C.; Duan, J.; Lee, G. J. *Mater. Chem.* **2005**, *15*, 1035. (f) Tsuboyama, A.; Iwawaki, H.; Furugori, M.; Mukaide, T.; Kamatani, J.; Igawa, S.; Moriyama, T.; Miura, S.; Takiguchi, T.; Okada, S.; Hoshino, M.; Ueno, K. *J. Am. Chem. Soc.* **2003**, *125*, 12971.

transitions in the free flzH compound, as expected for a metal complex with three such ligands. Strong absorption bands at lower energy ( $\lambda = 320\text{--}420\text{ nm}$ ,  $\epsilon > 1 \times 10^4\text{ M}^{-1}\text{ cm}^{-1}$ ) are assigned to a combination of singlet and triplet MLCT transitions, since their energy corresponds quite closely to a redox gap measured by solution electrochemistry ( $\lambda_{\text{max}} = 357\text{ nm}$ ,  $3.47\text{ eV}$ ;  $\Delta E_{1/2}^{\text{redox}} = E_{1/2}^{\text{ox}} - E_{1/2}^{\text{red}} = 3.41\text{ V}$ ). The intensities of these MLCT transitions are higher than their counterparts in either the *fac*-Ir(ppz)<sub>3</sub> or *fac*-Ir(ppy)<sub>3</sub> spectra, most likely due to the high oscillator strength of the fluorenyl chromophore. Much weaker absorption bands at still lower energy ( $\lambda = 420\text{--}485\text{ nm}$ ,  $\epsilon < 100\text{ M}^{-1}\text{ cm}^{-1}$ ) can be observed in concentrated solutions of the complex<sup>32</sup> and are assigned to <sup>3</sup>LC transitions that have enhanced intensity due to mixing with the <sup>1</sup>MLCT states.

The *fac*-Ir(flz)<sub>3</sub> complex displays an intense, structured emission in solution at 77 K ( $E_{0-0} = 480\text{ nm}$ ,  $2.58\text{ eV}$ ) with a lifetime of  $50\text{ }\mu\text{s}$  (Figure 2). The well-defined vibronic fine structure in the emission spectrum of *fac*-Ir(flz)<sub>3</sub> is indicative of a predominant <sup>3</sup>LC character in the excited state. The difference in the emission energy of *fac*-Ir(flz)<sub>3</sub> relative to *fac*-Ir(ppz)<sub>3</sub> ( $E_{0-0}^{\text{Ir(ppz)}_3} - E_{0-0}^{\text{Ir(flz)}_3} = 0.42\text{ eV}$ ) closely corresponds to the difference in triplet energy between their respective ligands (flzH ligand,  $E_{0-0} = 445\text{ nm}$ ,  $2.79\text{ eV}$ ;<sup>32</sup>  $E_{0-0}^{\text{ppzH}} - E_{0-0}^{\text{flzH}} = 0.47\text{ eV}$ ). More importantly, the PL efficiency of *fac*-Ir(flz)<sub>3</sub> at room temperature is high ( $\Phi = 0.38$ ) and the measured lifetime is  $37\text{ }\mu\text{s}$ . The radiative ( $k_r$ ) and nonradiative ( $k_{\text{nr}}$ ) decay rates estimated from the lifetime and PL efficiency<sup>33</sup> are  $1.0 \times 10^4\text{ s}^{-1}$  and  $2.0 \times 10^4\text{ s}^{-1}$ , respectively. These rates are an order of magnitude lower than those reported for both blue and green emissive cyclometalated Ir complexes, such as those illustrated in Figure 1.<sup>2,12,18a</sup> The low radiative rate for *fac*-Ir(flz)<sub>3</sub> is consistent with a low level of <sup>1</sup>MLCT character in the lowest excited state and is due to the large separation between the <sup>1</sup>MLCT and ligand triplet energies ( $\Delta E_{1/2}^{\text{redox}} - E_{0-0}^{\text{flzH}} = 0.62\text{ eV}$ ). Note that the corresponding energy separation for *fac*-Ir(ppy)<sub>3</sub> is small ( $0.13\text{ eV}$ ), and thus, the radiative rate for this species is high ( $k_r = 7.5 \times 10^5\text{ s}^{-1}$ ).<sup>23b</sup> A small <sup>1</sup>MLCT character in the lowest energy excited state of *fac*-Ir(flz)<sub>3</sub> relative to *fac*-Ir(ppz)<sub>3</sub> is also expected, since the fluorenyl substituent markedly lowers the <sup>3</sup>LC energy without decreasing the <sup>1</sup>MLCT level to the same extent. A correlation between the radiative rate and the separation of <sup>1</sup>MLCT and ligand triplet state energies was similarly observed for a series of related (C $\wedge$ N)<sub>2</sub>Ir(L $\wedge$ X) complexes.<sup>19</sup>

The *fac*-Ir(flz)<sub>3</sub> complex shows a negligible rigidochromic shift, in contrast to what is observed when comparing the room temperature and 77 K PL spectra of *fac*-Ir(ppy)<sub>3</sub> (Figure 2). The magnitude of the rigidochromic shift is also related to the degree of <sup>1</sup>MLCT character in the excited state.<sup>31f,34</sup> Molecular reorientation of the solvent dipoles enables a complex to reach a fully relaxed geometry in the excited

state at room temperature, whereas the solvent dipoles are unperturbed in the rigid matrix at low temperature. Since the formation of MLCT excited states involves substantial charge redistribution, such transitions typically display hypsochromic shifts upon going from a room temperature fluid solution to a 77 K glass. In contrast, excited states that are principally ligand based, e.g.,  $\pi\text{--}\pi^*$  states, generally have low levels of charge redistribution and, thus, give very small rigidochromic shifts. Hence, a greater MLCT character in the excited state of the Ir complexes is expected to lead to a large rigidochromic shift. For example, a clear correlation between the degree of MLCT character in the excited state and the magnitude of the rigidochromic shift was demonstrated for (C $\wedge$ N)<sub>2</sub>Ir(L $\wedge$ X) complexes.<sup>19</sup> Therefore, the absence of a rigidochromic shift for *fac*-Ir(flz)<sub>3</sub> provides further support that the excited state is largely <sup>3</sup>LC in character.

**Cyclometalated Carbene Ligands for Near-UV Phosphorescence.** Although modification of *fac*-Ir(ppz)<sub>3</sub> with the fluorenyl group leads to a complex that is highly emissive at room temperature, the emission energy of *fac*-Ir(flz)<sub>3</sub> is lower than that of compounds such as *fac*-Ir(F<sub>2</sub>ppy)<sub>3</sub> (Figure 1). For some applications, complexes with higher emission energy are highly desirable. Thus, a potentially more attractive approach to achieving efficient blue phosphorescence from cyclometalated Ir complexes at room temperature would be to increase the energy of the nonemissive excited state so that thermal population to it is inhibited, as shown in Figure 3b. The key to this approach is to design cyclometalating ligands that destabilize the NR state. If this state is a metal-localized, ligand field state, strengthening the metal–ligand bonds will destabilize its energy, since the state is comprised of antibonding counterparts to the metal–ligand bonding orbitals. Of the number of potential ligand choices that could have stronger ligand fields than pyrazolyl, the ligand type used here is an *N*-heterocyclic carbene (NHC). The syntheses of NHC ligand precursors are well-known,<sup>35</sup> making access to the complexes straightforward. The NHC ligands form very strong bonds with transition metals,<sup>36</sup> which will shift the metal–carbene antibonding orbitals to high energy, thereby decreasing or eliminating decay through the ligand field state. Specifically, the two NHC ligands studied here are 1-phenyl-3-methylimidazolin-2-ylidene (pmi) and 1-phenyl-3-methylbenzimidazolin-2-ylidene (pmb) (see Scheme 1). The carbene moiety is a neutral, two electron donor ligand, which makes the cyclometalated ligand a bidentate monoanionic ligand (C $\wedge$ C: is used here as a general abbreviation for a cyclometalated carbene ligand), similar to the C $\wedge$ N ligands that have been used to make stable iridium trischelates. An earlier example of triscyclometalated carbene complexes, Ir(C $\wedge$ C:)<sub>3</sub>, was reported in 1980 by Lappert et. al. (see Ir–Lappert in Scheme 1).<sup>37</sup> While an X-ray structure was given for this particular

(32) See the Supporting Information.

(33) The equations  $k_r = \Phi/\tau$  and  $k_{\text{nr}} = (1 - \Phi)/\tau$  were used to calculate the radiative ( $k_r$ ) and nonradiative ( $k_{\text{nr}}$ ) decay rates, where  $\Phi$  is the quantum efficiency and  $\tau$  is the luminescence lifetime of the sample at room temperature.

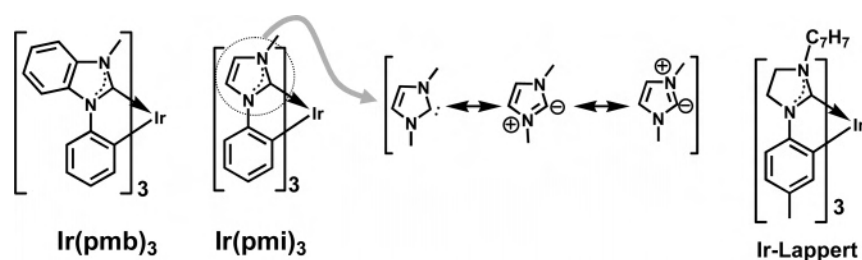
(34) Cummings, S. D.; Eisenberg, R. *J. Am. Chem. Soc.* **1996**, *118*, 1949.

(35) (a) Bourissou, D.; Guerret, O.; Gabbai, F. P.; Bertrand, G. *Chem. Rev.* **2000**, *100*, 39. (b) Klapars, A.; Antilla, J. C.; Huang, X.; Buchwald, S. L. *J. Am. Chem. Soc.* **2001**, *123*, 7727–7729.

(36) Nemcsok, D.; Wichmann, K.; Frenking, G. *Organometallics* **2004**, *23*, 3640.

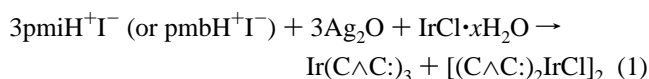


Scheme 1

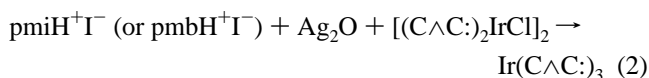


complex, to our knowledge, no photophysical data have been reported for these types of species.<sup>38</sup>

The  $\text{Ir(C}^{\wedge}\text{C:)}_3$  complexes were prepared by a modification of the method used to prepare the  $\text{Ir(C}^{\wedge}\text{N)}_3$  analogues.<sup>39</sup> A stoichiometric amount of imidazolium ( $\text{pmiH}^+$ ) or benzimidazolium ( $\text{pmbH}^+$ ) iodide salts, silver(I) oxide, and iridium(III) chloride hydrate were refluxed in a 2-ethoxyethanol solution to give a mixture of *fac*- and *mer*- $\text{Ir(C}^{\wedge}\text{C:)}_3$  complexes in low yield (<10%) along with a product formulated as  $[(\text{C}^{\wedge}\text{C:})_2\text{IrCl}]_2$  (eq 1).<sup>40</sup> The  $[(\text{C}^{\wedge}\text{C:})_2\text{IrCl}]_2$



complex can then be treated with additional  $\text{pmiH}^+$  or  $\text{pmbH}^+$  and silver(I) oxide in 1,2-dichloroethane to form a mixture of *fac*- and *mer*- $\text{Ir(C}^{\wedge}\text{C:)}_3$  complexes (eq 2). The



silver(I) oxide has several potential roles in these reactions: to deprotonate the imidazolium salt and stabilize the resultant carbene ligand, to abstract the chloride ligand from the Ir salt, and to serve as a transmetalating agent.<sup>41,17a</sup> To date, we have been unable to optimize eq 1 to give a high yield of any particular cyclometalated product. The synthesis using eq 2 also gives a mixture of the facial or meridional isomers of the  $\text{Ir(C}^{\wedge}\text{C:)}_3$  complex (see the Experimental Section). The *mer*-isomers of the  $\text{Ir(C}^{\wedge}\text{C:)}_3$  complexes do not convert to their facial isomers upon photolysis but, instead, eventually decompose under long term UV exposure. Likewise, the facial isomers also decompose during extensive irradiation; hence, it is not possible to determine which configuration of the  $\text{Ir(C}^{\wedge}\text{C:)}_3$  complexes is the thermodynamically favored isomer. Pure samples of *fac*- and *mer*- $\text{Ir(C}^{\wedge}\text{C:)}_3$  isomers were, therefore, isolated by either column chromatography

or selective precipitation/crystallization, a procedure aided by the lower solubility of the *fac*-isomers. These synthetic difficulties are in contrast to the case of the previously developed high yield synthesis for  $\text{Ir(C}^{\wedge}\text{N)}_3$  complexes using the chloride bridged dimer,  $(\text{C}^{\wedge}\text{N})_2\text{Ir}(\mu\text{-Cl})_2\text{Ir(C}^{\wedge}\text{N})_2$ .<sup>18a</sup> The *mer*-isomers of the  $\text{Ir(C}^{\wedge}\text{N)}_3$  complexes are the kinetically favored species and can be readily converted to the facial isomers, either by thermal or photochemical means, with minimal decomposition. We presume that the failure to interconvert the *fac*- and *mer*-isomers of the  $\text{Ir(C}^{\wedge}\text{C:)}_3$  complexes is principally due to  $\text{Ir-C}_{\text{carbene}}$  bonds being stronger than  $\text{Ir-N}$  bonds, making the partial ligand dissociation that is necessary for isomerization more difficult for the  $\text{Ir(C}^{\wedge}\text{C:)}_3$  complexes than for their  $\text{C}^{\wedge}\text{N}$  counterparts.

Single crystals of *fac*- $\text{Ir(pmb)}_3$  and *mer*- $\text{Ir(pmb)}_3$  were grown from a methanol/dichloromethane solution and characterized using X-ray crystallography. Molecular structures of *fac*- $\text{Ir(pmb)}_3$  and *mer*- $\text{Ir(pmb)}_3$  are shown in Figure 5. Selected bond distances and angles of the complexes are provided in Table 1, along with those of *mer*- $\text{Ir(ppz)}_3$ , for which structural data were taken from the literature.<sup>18a</sup> All of the complexes analyzed here have the three cyclometalating ligands in a pseudo-octahedral coordination geometry around the iridium center. The  $\text{C}^{\wedge}\text{C:}$  ligands in both *fac*- and *mer*- $\text{Ir(pmb)}_3$  are twisted from planarity around the bridging  $\text{C}_{\text{phenyl}}\text{-N}_{\text{carbene}}$  bond. The distortion is presumably due to steric repulsion between adjacent hydrogen atoms on the phenyl and benzimidazolyl moieties. The twist is smaller in the *fac*-isomer (dihedral angles are between 1 and 10°) than in the *mer*-isomer (dihedral angles vary between 5 and 27°). This variation in ligand distortion is most likely due to crystal packing effects.

It is instructive to compare the Ir coordination environment of the facial isomer of  $\text{Ir(pmb)}_3$  to that of the same isomer for  $\text{Ir(ppz)}_3$ . In *fac*- $\text{Ir(pmb)}_3$ , the average  $\text{Ir-C}_{\text{carbene}}$  distance (2.026(7) Å) is significantly shorter than the average  $\text{Ir-N}$  distance in *fac*- $\text{Ir(ppz)}_3$  (2.124(5) Å). The short distance in *fac*- $\text{Ir(pmb)}_3$  suggests that the carbene moiety is more strongly bound to the Ir than the pyrazolyl ligand. Moreover, the average  $\text{Ir-C}_{\text{phenyl}}$  distance (2.081(7) Å) in *fac*- $\text{Ir(pmb)}_3$  is longer than the average  $\text{Ir-C}_{\text{phenyl}}$  distance in *fac*- $\text{Ir(ppz)}_3$  (2.021(6) Å), suggesting that the carbene is a stronger field ligand than the pyrazolyl. The bonding parameters found for the meridional isomer of the complex support this view as well. In *mer*- $\text{Ir(pmb)}_3$ , the bond length of  $\text{Ir-C}_{\text{aryl}}$  trans to benzimidazolyl ( $\text{Ir-C2} = 2.078(4)$  Å) is greater than the bond length of  $\text{Ir-C}_{\text{aryl}}$  trans to the pyrazolyl group in *mer*- $\text{Ir(ppz)}_3$  ( $\text{Ir-C3} = 1.993(2)$  Å), illustrating the stronger trans

(37) Hitchcock, P. B.; Lappert, M. F.; Terreros, P. J. *Organomet. Chem.* **1982**, 239, C26.

(38) For a recent example of a related luminescent Ru complex with a noncyclometalated NHC ligand, see: Son, S. U.; Park, K. H.; Lee, Y.-S.; Kim, B. Y.; Choi, C. H.; Lah, M. S.; Jang, Y. H.; Jang, D.-J.; Chung, Y. K. *Inorg. Chem.* **2004**, 43, 6896–6898.

(39) Lamansky, S.; Djurovich, P. I.; Murphy, D.; Abdel-Razaq, F.; Kwong, R.; Tsyba, I.; Bortz, M.; Mui, B.; Bau, R.; Thompson, M. E. *Inorg. Chem.* **2001**, 40, 1704–1711.

(40) The formulation of the  $[(\text{C}^{\wedge}\text{C:})_2\text{IrCl}]_2$  complexes as  $\mu$ -dichlorobridged dimers is based on their relatively simple  $^1\text{H}$  NMR spectra and by analogy to the  $[(\text{C}^{\wedge}\text{N})_2\text{IrCl}]_2$  complexes. In addition, the  $[(\text{C}^{\wedge}\text{C:})_2\text{IrCl}]_2$  complexes can be treated with 4,4'-di-*tert*-butyl-2,2'-bipyridine to form cationic complexes with the general formula  $[(\text{C}^{\wedge}\text{C:})_2\text{Ir}(\text{N}^{\wedge}\text{N})]^+$  (unpublished results).

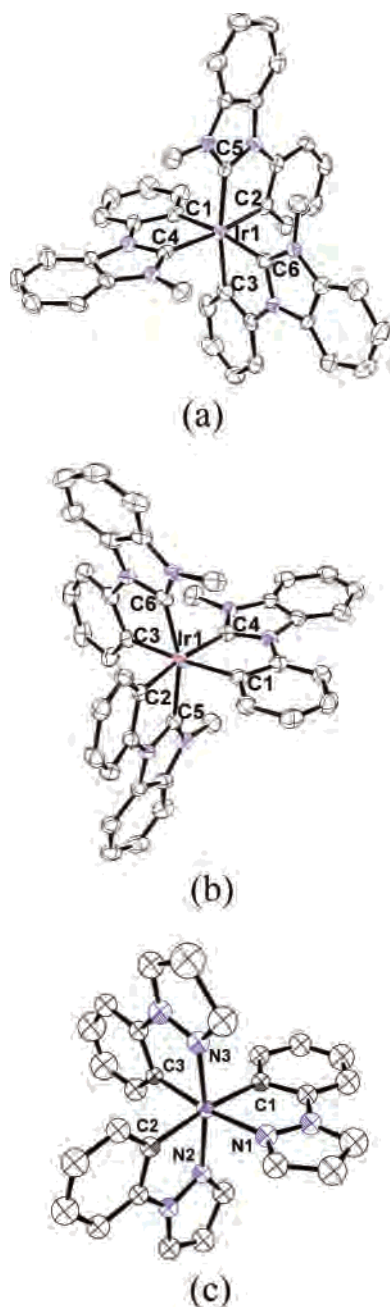


**Figure 5.** Thermal ellipsoid (ORTEP) plots of (a) *fac*-Ir(pmb)<sub>3</sub>, (b) *mer*-Ir(pmb)<sub>3</sub>, and (c) *mer*-Ir(ppz)<sub>3</sub>.<sup>18a</sup> The hydrogen atoms have been omitted for clarity. The atom numbering used in Table 1 is shown.

influence of the carbene ligand over that of pyrazolyl. The lengths of the mutually trans Ir–C<sub>aryl</sub> bond (Ir–C1 and Ir–C3, average (av) = 2.093(4) Å) in *mer*-Ir(pmb)<sub>3</sub> are slightly longer than those in *mer*-Ir(ppz)<sub>3</sub> (av = 2.040(2) Å), indicating greater electron donation from the carbene ligand than from the pyrazolyl moiety. The structures of both isomers of Ir(pmb)<sub>3</sub> are consistent with a strong trans influence of a formally neutral carbene ligand. The bond length differences suggest that the cyclometalated carbenes are stronger field ligands than their pyrazolyl or pyridyl counterparts, and therefore, the Ir(C $\wedge$ C:)<sub>3</sub> complexes should have high energy ligand field states.

The Ir(pmi)<sub>3</sub> and Ir(pmb)<sub>3</sub> complexes display electrochemical and absorption characteristics comparable to those

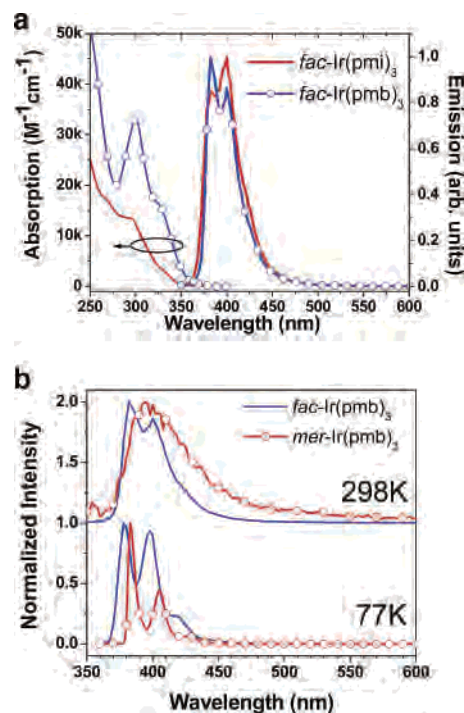


**Figure 6.** (a) Absorption and emission spectra for *fac*-Ir(pmi)<sub>3</sub> and *fac*-Ir(pmb)<sub>3</sub> in CH<sub>2</sub>Cl<sub>2</sub> at room temperature and (b) emission spectra of *fac*- and *mer*-Ir(pmb)<sub>3</sub> in 2-MeTHF at room temperature and 77 K.

of *fac*-Ir(ppz)<sub>3</sub>. The data are consistent with the Ir(C $\wedge$ C:)<sub>3</sub> complexes having both low HOMO and high LUMO energies. The *fac*-isomers undergo reversible oxidation (*fac*-Ir(pmi)<sub>3</sub>,  $E_{1/2}^{ox} = 0.22$  V; *fac*-Ir(pmb)<sub>3</sub>,  $E_{1/2}^{ox} = 0.48$  V) and no observable reduction within the accessible solvent window, similar to the data shown in Figure 2 for *fac*-Ir(ppz)<sub>3</sub>. The *mer*-isomers are easier to oxidize than their *fac* counterparts (*mer*-Ir(pmi)<sub>3</sub>,  $E_{1/2}^{ox} = 0.14$  V; *mer*-Ir(pmb)<sub>3</sub>,  $E_{1/2}^{ox} = 0.31$  V), and an irreversible reduction can be observed in *mer*-Ir(pmb)<sub>3</sub> at –3.2 V. The absorption spectra show strong bands at high energy ( $\lambda < 270$  nm,  $\epsilon > 2 \times 10^4$  M<sup>-1</sup> cm<sup>-1</sup>) that are assigned to ligand  $\pi$ – $\pi^*$  transitions of the cyclometalating ligands, whereas weaker bands at lower energy ( $\lambda = 270$ –360 nm,  $\epsilon \sim 10^4$  M<sup>-1</sup> cm<sup>-1</sup>) are ascribed to MLCT transitions (Figure 6). A weak, low energy band is also present in both complexes ( $\lambda = 380$  nm,  $\epsilon \sim 100$  M<sup>-1</sup> cm<sup>-1</sup>) and is assigned to a perturbed <sup>3</sup>LC transition. The *fac*- and *mer*-isomers have similar absorption band shapes in each of the respective complexes. An interesting feature of *fac*-Ir(pmi)<sub>3</sub> and *fac*-Ir(pmb)<sub>3</sub> complexes is the small difference in their MLCT absorption energies. This similarity is surprising in view of the large decrease in the MLCT absorption energy (ca. 0.3 eV) that occurs when the  $\pi$ -system of the pyridyl ring in (ppy)<sub>2</sub>Ir(acac) is expanded by adding a fused phenyl ring to form (pq)<sub>2</sub>Ir(acac).<sup>2</sup> Apparently, the minor variance of the MLCT energy upon extension of the  $\pi$ -system of the imidazolyl–carbene moiety is due to poor conjugation of the phenyl and benzimidazolyl fragments, such that the phenyl and carbene moieties behave as independent chromophores.

All of the Ir(C $\wedge$ C:)<sub>3</sub> complexes display intense emission at 77 K in the near-UV spectrum and, notably, also luminesce



**Table 2.** Photophysical Parameters for Ir(C $\wedge$ N)<sub>3</sub> and Ir(C $\wedge$ C)<sub>3</sub> Complexes<sup>a</sup>

	$\phi_{\text{PL}}$	$\tau$ ( $\mu\text{s}$ ) 300 K	$k_{\text{r}}$ ( $10^4 \text{ s}^{-1}$ )	$k_{\text{nr}}$ ( $10^6 \text{ s}^{-1}$ )	$\tau$ ( $\mu\text{s}$ ) 77 K	$\phi$ ( $\mu\text{s}$ ) 77 K (polystyrene)
<i>fac</i> -Ir(flz) <sub>3</sub>	0.38	37	1.0	0.020	50	48
<i>fac</i> -Ir(pmi) <sub>3</sub>	0.02	0.40	5	2	6.8	
<i>mer</i> -Ir(pmi) <sub>3</sub>	0.05	0.62	8	2	2.4	3.4
<i>fac</i> -Ir(pmb) <sub>3</sub>	0.04	0.22	18	4	3.1	1.1
<i>mer</i> -Ir(pmb) <sub>3</sub>	0.002	0.015	13	65	2.4	1.0

<sup>a</sup>The values listed are for 2-MeTHF solutions at room temperature, unless otherwise noted.

at room temperature in fluid solution (Figure 6). The quantum efficiencies and lifetimes for the Ir(C $\wedge$ C)<sub>3</sub> complexes are given in Table 2. The excited state properties of the Ir(C $\wedge$ C)<sub>3</sub> complexes are related to those of the Ir(C $\wedge$ N)<sub>3</sub> analogues in that both types of species emit from perturbed <sup>3</sup>LC states. The emission spectra at 77 K are highly structured (vibronic spacings of ca. 1300 cm<sup>-1</sup>) and have luminescent lifetimes between 2 and 7  $\mu\text{s}$ . The emission spectra of the *fac*- and *mer*-isomers are very similar in appearance (Figure 6), unlike the distinctly different line shapes seen for the emission spectra of the *fac*- and *mer*-isomers of Ir(C $\wedge$ N)<sub>3</sub> complexes.<sup>18a</sup> The Ir(pmi)<sub>3</sub> and Ir(pmb)<sub>3</sub> complexes have high emission energies that are nearly identical in value ( $E_{0-0} = 380 \text{ nm}$ , 3.26 eV). These energies approach the value for the triplet state of *N,N*-diethylaniline ( $E_{0-0} = 370 \text{ nm}$ , 3.35 eV).<sup>42</sup> The high emission energies of the Ir(C $\wedge$ C)<sub>3</sub> complexes in conjunction with their low oxidation potentials imply that these materials have extremely high reduction potentials when in the excited state ( $E_{1/2}^{+/0*} \approx E_{1/2}^{\text{ox}} - E_{0-0}$ ; *fac*-Ir(pmi)<sub>3</sub>,  $E_{1/2}^{+/0*} = -3.04 \text{ V}$ ; *fac*-Ir(pmb)<sub>3</sub>,  $E_{1/2}^{+/0*} = -2.78 \text{ V}$ ). The potent reducing ability of the Ir(C $\wedge$ C)<sub>3</sub> complexes in their excited states could make these materials interesting candidates for use in photoinduced electron-transfer studies.

The PL efficiencies at room temperature for the Ir(C $\wedge$ C)<sub>3</sub> complexes are low (0.002–0.05) but, nevertheless, higher than those for their pyrazolyl counterparts. The radiative and nonradiative decay rates of *fac*-Ir(pmi)<sub>3</sub> ( $k_{\text{r}} = 5 \times 10^4 \text{ s}^{-1}$ ,  $k_{\text{nr}} = 2 \times 10^6 \text{ s}^{-1}$ ) are comparable to those of *fac*-Ir(pmb)<sub>3</sub> ( $k_{\text{r}} = 1.8 \times 10^5 \text{ s}^{-1}$ ,  $k_{\text{nr}} = 4 \times 10^6 \text{ s}^{-1}$ ). The *mer*-isomer of Ir(pmb)<sub>3</sub> has a lower PL efficiency and a higher nonradiative decay rate than its facial analogue, which is similar to what was found for the corresponding properties in the *fac*- and *mer*-isomers of Ir(C $\wedge$ N)<sub>3</sub> complexes.<sup>18</sup> The radiative rates for the Ir(C $\wedge$ C)<sub>3</sub> complexes are higher than that for *fac*-Ir(flz)<sub>3</sub> but less than that for *fac*-Ir(ppy)<sub>3</sub>, consistent with an intermediate degree of <sup>1</sup>MLCT character in the excited states of the Ir(C $\wedge$ C)<sub>3</sub> complexes. The moderate rigidochromic shifts for the Ir(C $\wedge$ C)<sub>3</sub> complexes (see Figure 6) also suggest that their excited states have more MLCT character than those of *fac*-Ir(flz)<sub>3</sub> (largely <sup>3</sup>LC based) but less than those of *fac*-Ir(ppy)<sub>3</sub>. The greater <sup>1</sup>MLCT character in the excited

states of the Ir(C $\wedge$ C)<sub>3</sub> complexes relative to *fac*-Ir(flz)<sub>3</sub> is presumably due to the <sup>1</sup>MLCT and <sup>3</sup>LC levels being closer in energy and, thus, more effectively mixed in the Ir(C $\wedge$ C)<sub>3</sub> complexes than in *fac*-Ir(flz)<sub>3</sub>.

The fact that near-UV emission is observed at room temperature from the Ir(C $\wedge$ C)<sub>3</sub> complexes suggests that the nonemissive excited state for these complexes has been significantly destabilized relative to the similar state in *fac*-Ir(ppz)<sub>3</sub>. However, the Ir(C $\wedge$ C)<sub>3</sub> complexes still undergo nonradiative decay to a greater extent than *fac*-Ir(flz)<sub>3</sub>, as evidenced by their high nonradiative rates and low PL efficiencies. The high nonradiative decay rates for the Ir(C $\wedge$ C)<sub>3</sub> complexes indicate that a thermally accessible NR state is still present in these species. Thermal activation to this state can be largely eliminated by cooling the compounds to low temperature, and the measured lifetimes under these conditions are close to the radiative lifetimes. An alternative means to suppress the nonradiative decay processes at room temperature is to immobilize the complexes in a rigid matrix. Accordingly, when the Ir(C $\wedge$ C)<sub>3</sub> complexes are dispersed in polystyrene, the lifetimes increase by nearly an order of magnitude at room temperature (see Table 2). A similar increase in radiative lifetime for Ru(II) and Os(II) tris-diimine complexes in polymeric matrices was previously reported and has been attributed to the inhibition of ligand field decay pathways in the rigid media.<sup>25,43</sup> The long lifetimes obtained in polystyrene for the Ir(C $\wedge$ C)<sub>3</sub> complexes imply that the luminance efficiencies at room temperature are much higher in the polymer matrix ( $\Phi > 0.1$ –0.2) than values measured in fluid solution. This behavior is noteworthy with regards to the use of the Ir(C $\wedge$ C)<sub>3</sub> complexes as phosphorescent dopants in applications such as OLEDs, since it suggests that the PL efficiencies in doped films are similarly quite high in value. If the luminance efficiencies were to remain low in the solid state, the Ir(C $\wedge$ C)<sub>3</sub> complexes would be of little use as phosphorescent emitters. Consequently, we have fabricated OLEDs using the Ir(C $\wedge$ C)<sub>3</sub> complexes as dopants and have obtained high external quantum efficiencies (>5%), consistent with values of  $\Phi > 0.2$ . A detailed study of these devices is currently underway and will be presented in a future report.<sup>44</sup>

## Conclusion

The approach to tuning the photophysical properties of cyclometalated Ir complexes investigated here involved the control of the relative energies of emissive and non-emissive excited states. The starting point for this work was a high triplet energy Ir complex, i.e., *fac*-Ir(ppz)<sub>3</sub>, that gives no measurable emission at room temperature. By increasing the energy separation between emissive and nonemissive states, nonradiative decay rates could be decreased, leading to substantially improved luminescent quantum yields. This was demonstrated either by lowering the energy of the emitting

(41) (a) Wang, H. M. J.; Lin, I. J. B. *Organometallics* **1998**, *17*, 972–975.  
(b) Chianese, A. R.; Li, X.; Janzen, M. C.; Faller, J. W.; Crabtree, R. H. *Organometallics* **2003**, *22*, 1663–1667.  
(42) Murov, S. L.; Carmichael, I.; Hug, G. L. *Handbook of Photochemistry*, 2nd ed.; Marcel Dekker: New York, 1993.

(43) Draxler, S. *J. Phys. Chem. A* **1999**, *103*, 4719.  
(44) Holmes, R.; Forrest, S. R.; Sajoto, T.; Tamayo, A.; Djurovich, P. I.; Thompson, M. E.; Brooks, J.; Tung, Y.-J.; D'Andrade, B. W.; Weaver, M. S.; Kwong, R. C.; Brown, J. J. *Appl. Phys. Lett.*, submitted for publication.

state, as in *fac*-Ir(flz)<sub>3</sub>, or by increasing the energies of the non-emissive states, as in the Ir(C $\wedge$ C:)<sub>3</sub> complexes. While the *fac*-Ir(flz)<sub>3</sub> complex has a markedly lower triplet state energy than the *fac*-Ir(flz)<sub>3</sub> complex, the Ir(C $\wedge$ C:)<sub>3</sub> complexes have higher triplet energies and display near-UV luminescence at room temperature. The next step in this study is to examine the temperature dependence of the photophysical properties of these materials. The temperature dependence of the emission lifetime and efficiency can be used to determine the relative energies and decay rates for both the emissive and nonemissive excited states of the NHC- and pyrazolyl-based materials. With this information in hand, we will be able to evaluate the nature of the nonradiative decay processes and design ligands and complexes that more effectively destabilize the non-emissive states, leading to higher luminance efficiencies. A detailed temperature dependent study is currently in progress.

## Experimental Section

Solvents and reagents for synthesis were purchased from Aldrich, Matrix Scientific, and EM Science and were used without further purification. IrCl<sub>3</sub>·*n*H<sub>2</sub>O was purchased from Next Chimica. *N,N*-Dimethylformamide (EM Science, anhydrous, 99.8%) and tetra-*n*-butylammonium hexafluorophosphate (TBAH) (Fluka, electrochemistry grade) were used for spectroscopic and electrochemical measurements. The syntheses of 1-[2-(9,9-dimethylfluorenyl)]pyrazole, 1-phenyl-3-methylimidazolium iodide, and 1-phenyl-3-methylbenzimidazolium iodide are given in the Supporting Information. The synthesis and characterization of *fac*-Ir(flz)<sub>3</sub>, *fac*- and *mer*-Ir(pmi)<sub>3</sub>, and *fac*- and *mer*-Ir(pmb)<sub>3</sub> are given below. All syntheses involving IrCl<sub>3</sub>·*n*H<sub>2</sub>O or any other Ir(III) species were carried out under an inert atmosphere.

**Synthesis of *fac*-Iridium(III) Tris(1-[2-(9,9-dimethylfluorenyl)]pyrazolyl-*N*,*C*<sup>3'</sup>), *fac*-Ir(flz)<sub>3</sub>.** The *fac*-Ir(flz)<sub>3</sub> complex was prepared using the same two step procedure as that used for *fac*-Ir(ppz)<sub>3</sub>.<sup>18a</sup> A fluorenylpyrazolyl-based Ir(III)  $\mu$ -dichloro-bridged dimer, [(flz)<sub>2</sub>IrCl]<sub>2</sub>, was synthesized in a 100 mL round-bottomed flask that was charged with iridium trichloride hydrate (0.250 g, 0.837 mmol), 1-[2-(9,9-dimethylfluorenyl)]pyrazole (0.500 g, 1.92 mmol), and 60 mL of a 2-ethoxyethanol–water mixture (3:1). The reaction mixture was stirred and heated with an oil bath at 110 °C for 16 h under nitrogen and then allowed to cool to ambient temperature. Addition of water gave the [(flz)<sub>2</sub>IrCl]<sub>2</sub> complex as a yellowish-white solid (0.415 g, 66%), which was used without further purification in the next step to prepare the diketonate complex.

In a 100 mL round-bottomed flask, the [(flz)<sub>2</sub>IrCl]<sub>2</sub> complex (0.250 g, 0.168 mmol), 2,4-pentanedione (0.036 mL, 0.352 mmol), and excess K<sub>2</sub>CO<sub>3</sub> were combined with 60 mL of 1,2-dichloroethane. The reaction mixture was stirred and heated with an oil bath at 90 °C for 16 h under nitrogen. After being cooled to ambient temperature, the reaction mixture was filtered to remove the insoluble salts and the solvent was removed from the filtrate under reduced pressure. Addition of methanol gave 0.248 g of a light yellow solid which was found to be (flz)<sub>2</sub>Ir(acac) (91% yield). <sup>1</sup>H NMR (360 MHz, CDCl<sub>3</sub>), ppm: 8.16 (dd, *J* = 2.9, 1.0 Hz, 2H), 7.69 (dd, *J* = 2.2, 0.73 Hz, 2H), 7.25–7.29 (m, 2H), 7.31–7.35 (m, 2H), 7.19 (s, 2H), 7.09–7.18 (m, 4H), 6.71 (dd, *J* = 2.9, 2.2 Hz, 2H), 6.54 (s, 2H), 5.23 (s, 1H), 1.40 (s, 6H), 1.38 (s, 12H).

A 50 mL round-bottomed flask was charged with the (flz)<sub>2</sub>Ir(acac) complex (0.100 g, 0.125 mmol), 1-[2-(9,9-dimethylfluor-

enyl)]pyrazole (0.036 g, 0.138 mmol), and 25 mL of glycerol. The reaction mixture was stirred and heated in an oil bath at 210–220 °C for 24 h under a nitrogen atmosphere. After being cooled to ambient temperature, distilled water was added to the reaction mixture and the precipitate was vacuum filtered and dried. The crude product was purified by flash column chromatography on silica gel using dichloromethane as the eluent to give pure *fac*-Ir(flz)<sub>3</sub> (0.0895 g, 75%). <sup>1</sup>H NMR (360 MHz, CDCl<sub>3</sub>), ppm: 8.1 (dd, *J* = 2.8, 0.5 Hz, 3H), 7.36 (dd, *J* = 6.7, 1.3 Hz, 3H), 7.29 (s, 3H), 7.28 (s, 3H), 7.26 (dd, *J* = 6.3, 1.5 Hz, 3H), 7.14 (ddd, *J* = 7.5, 7.4, 1.5 Hz, 3H), 7.10 (ddd, *J* = 7.4, 7.2, 1.3 Hz, 3H), 7.03 (dd, *J* = 2.1, 0.4 Hz, 3H), 6.41 (dd, *J* = 2.8, 2.2 Hz, 3H), 1.56 (s, 9H), 1.46 (s, 9H). <sup>13</sup>C (90.55 MHz, CDCl<sub>3</sub>), ppm: 153.74, 146.77, 143.75, 140.02, 138.47, 136.74, 136.55, 128.86, 126.54, 125.73, 124.87, 121.98, 119.88, 106.53, 105.55, 46.23, 28.03, 27.19. CHN Analysis Calcd: C, 66.85; H, 4.68; N, 8.66. Observed: C, 66.22; H, 4.52; N, 8.55.

**Synthesis of [(pmi)<sub>2</sub>IrCl]<sub>2</sub>.** A 100 mL round-bottomed flask was charged with silver(I) oxide (0.428 g, 1.85 mmol), 1-phenyl-3-methylimidazolium iodide (0.946 g, 3.31 mmol), iridium trichloride hydrate (0.301 g, 1.01 mmol), and 60 mL of 2-ethoxyethanol. The reaction mixture was stirred and heated with an oil bath at 120 °C for 15 h under nitrogen while protected from light with aluminum foil. The reaction mixture was cooled to ambient temperature, and the solvent was removed under reduced pressure. The black mixture was extracted with ca. 20 mL of dichloromethane, and the extract was reduced to a volume of ca. 2 mL. Addition of methanol gave an off-white solid, which was formulated as the dichlorobridged dimer on the basis of its relatively simple <sup>1</sup>H NMR spectrum, along with some unreacted ligand. <sup>1</sup>H NMR (250 MHz, CDCl<sub>3</sub>), ppm: 7.50 (d, *J* = 2.0 Hz, 4H), 7.07 (d, *J* = 2.0 Hz, 4H), 6.09 (dd, *J* = 7.8, 1.0 Hz, 4H), 6.63 (ddd, *J* = 7.5, 7.5, 1.4 Hz, 4H), 6.15 (ddd, *J* = 7.5, 7.5, 1.4 Hz, 4H), 3.87 (s, 12H). This product was used without further purification for the synthesis of the *fac*-Ir(pmi)<sub>3</sub>.

**Synthesis of *fac*-Iridium(III) Tris(1-phenyl-3-methylimidazolyl-2-ylidene-*C*,*C*<sup>2</sup>), *fac*-Ir(pmi)<sub>3</sub>.** A 50 mL round-bottomed flask was charged with silver(I) oxide (0.278 g, 1.20 mmol), 1-phenyl-3-methylimidazolium iodide (0.080 g, 0.280 mmol), [(pmi)<sub>2</sub>IrCl]<sub>2</sub> (0.108 g, 0.091 mmol), and 25 mL of 1,2-dichloroethane. The reaction mixture was stirred and heated with an oil bath at 77 °C for 15 h under nitrogen while protected from light with aluminum foil. The reaction mixture was cooled to ambient temperature and concentrated under reduced pressure. The dark residue was taken up in dichloromethane, and the silver(I) salts were removed by filtration through Celite. The resultant light brown solution was further purified by flash column chromatography on silica gel using dichloromethane as the eluent and was then reduced in volume to ca. 2 mL. Addition of methanol gave 0.010 g (8% yield) of the iridium complex as an off-white solid. <sup>1</sup>H NMR (360 MHz, CD<sub>2</sub>-Cl<sub>2</sub>), ppm: 7.43 (d, *J* = 2.0 Hz, 3H), 7.16 (dd, *J* = 7.7, 1.0 Hz, 3H), 6.89 (ddd, *J* = 8.0, 7.3, 1.5 Hz, 3H), 6.78 (d, *J* = 2.0 Hz, 3H), 6.71 (ddd, *J* = 8.0, 7.3, 1.5 Hz, 3H), 6.60 (dd, *J* = 7.2, 1.4 Hz, 3H). <sup>13</sup>C (90.55 MHz, CD<sub>2</sub>-Cl<sub>2</sub>), ppm: 176.77, 150.12, 148.05, 137.80, 125.02, 120.73, 120.56, 114.71, 110.42, 36.95. CHN Analysis Calcd: C, 54.28; H, 4.10; N, 12.66. Observed: C, 54.09; H, 3.83; N, 12.47.

**Synthesis of *mer*-Iridium(III) Tris(1-phenyl-3-methylimidazolyl-2-ylidene-*C*,*C*<sup>2</sup>), *mer*-Ir(pmi)<sub>3</sub>.** A 50 mL round-bottomed flask was charged with silver(I) oxide (0.076 g, 0.328 mmol), 1-phenyl-3-methylimidazolium iodide (0.109 g, 0.381 mmol), iridium trichloride hydrate (0.029 g, 0.097 mmol), and 20 mL of 2-ethoxyethanol. The reaction mixture was stirred and heated with an oil bath at 120 °C for 15 h under nitrogen while protected from

light with aluminum foil. The reaction mixture was cooled to ambient temperature and concentrated under reduced pressure. Filtration through Celite, using dichloromethane as the eluent, was performed to remove the silver(I) salts. A white solid was obtained after removing the solvent in vacuo and was washed with methanol to give 0.016 g (24% yield) of the meridional tris-iridium complex as a white solid.  $^1\text{H}$  NMR (360 MHz,  $\text{CDCl}_3$ ), ppm: 7.42 (d,  $J = 2.0$  Hz, 1H), 7.37 (d,  $J = 2.0$  Hz, 1H), 7.28 (d,  $J = 2.0$  Hz, 1H), 6.9–7.2 (m, 3H), 6.78–6.85 (m, 3H), 6.5–6.75 (m, 3H), 3.04 (s, 1H), 3.02 (s, 1H), 2.95 (s, 1H).  $^{13}\text{C}$  (90.55 MHz,  $\text{CDCl}_3$ ), ppm: 175.08, 173.62, 172.46, 151.43, 150.09, 148.87, 148.07, 147.44, 146.69, 139.76, 139.54, 137.27, 124.76, 124.71, 124.50, 124.33, 120.57, 120.40, 119.98, 119.66, 119.44, 119.39, 114.13, 114.11, 114.08, 110.07, 109.48, 36.99, 36.93, 35.87. CHN Analysis Calcd: C, 54.28; H, 4.10; N, 12.66. Observed: C, 54.25; H, 3.77; N, 12.44.

**Synthesis of  $[(\text{pmb})_2\text{IrCl}]_2$ .** A 100 mL round-bottomed flask was charged with silver(I) oxide (5.590 g, 24.1 mmol), 1-phenyl-3-methylbenzimidazolium iodide (6.756 g, 20.1 mmol), iridium trichloride hydrate (1.50 g, 5.02 mmol), and 50 mL of 2-ethoxyethanol. The reaction mixture was stirred and heated with an oil bath at 120 °C for 24 h under nitrogen while protected from light with aluminum foil. The reaction mixture was cooled to ambient temperature and concentrated under reduced pressure. Flash column chromatography on Celite using dichloromethane as the eluent was performed to remove the silver(I) salts. A brown oil was obtained, and addition of ethanol gave a light brown solid. The brownish solid was filtered and washed with ethanol. It was further purified by flash column chromatography on silica gel using dichloromethane as the eluent to give a yellowish solid product (0.412 g, 12.7% yield), which was formulated as  $[(\text{pmb})_2\text{IrCl}]_2$  based on  $^1\text{H}$  NMR spectral features that are similar to those for  $[(\text{pmi})_2\text{IrCl}]_2$ .  $^1\text{H}$  NMR (360 MHz,  $\text{CDCl}_3$ ), ppm: 8.18 (m, 4H), 7.62 (dd,  $J = 7.9, 1.2$  Hz, 4H), 7.52 (m, 4H), 7.30 (m, 4H), 6.78 (ddd,  $J = 8.3, 7.8, 1.3$  Hz, 4H), 6.38 (ddd,  $J = 8.2, 7.6, 1.1$  Hz, 4H), 6.24 (dd,  $J = 7.6, 1.3$  Hz, 4H), 3.78 (s, 12H).

**Synthesis of Iridium(III) Tris(1-phenyl-3-methylbenzimidazol-2-ylidene- $C, C^2$ ),  $\text{Ir}(\text{pmb})_3$ .** A 50 mL round-bottomed flask was charged with silver(I) oxide (0.0886 g, 0.382 mmol), 1-phenyl-3-methylbenzimidazolium iodide (0.225 g, 0.669 mmol),  $[(\text{pmb})_2\text{IrCl}]_2$  (0.412 g, 0.319 mmol), and 25 mL of 1,2-dichloroethane. The reaction mixture was stirred and heated with an oil bath at 95 °C for 24 h under nitrogen while protected from light with aluminum foil. The reaction mixture was cooled to ambient temperature and concentrated under reduced pressure. Flash column chromatography on 50:50 Celite and silica gel using dichloromethane as the eluent was performed to give 0.514 g of a mixture of meridional and facial  $\text{Ir}(\text{pmb})_3$  (3:1) as an off white solid. Column chromatography using ethyl acetate/hexanes (20:80) as the eluent was performed to give 0.400 g of predominantly *mer*- $\text{Ir}(\text{pmb})_3$  with some facial impurity (77% yield). The remaining *fac*- $\text{Ir}(\text{pmb})_3$  was eluted using ethyl acetate/hexanes (40:60) to give 0.110 g (21% yield) of pure *fac*- $\text{Ir}(\text{pmb})_3$ . Repeated column chromatography was required to obtain *mer*- $\text{Ir}(\text{pmb})_3$  free of the *fac* impurity.

(A) *fac*- $\text{Ir}(\text{pmb})_3$ .  $^1\text{H}$  NMR (360 MHz,  $\text{CDCl}_3$ ), ppm: 8.08 (d,  $J = 8.2$  Hz, 3H), 7.86 (d,  $J = 7.8$  Hz, 3H), 7.24 (ddd,  $J = 8.8, 6.9, 1.3$  Hz, 3H), 7.15 (ddd,  $J = 7.7, 8.06, 0.85$  Hz, 3H), 7.12 (d,  $J = 1.1$  Hz, 2H), 7.09 (d,  $J = 1.1$  Hz, 1H), 7.05 (ddd,  $J = 8.2, 7.0, 1.6$  Hz, 3H), 6.72 (ddd,  $J = 7.7, 7.1, 1.1$  Hz, 3H), 6.65 (dd,  $J = 7.3$  Hz, 3H) 3.22 (s, 9H).  $^{13}\text{C}$  (90.55 MHz,  $\text{CDCl}_3$ ), ppm: 189.58, 148.75, 148.65, 137.02, 136.31, 132.63, 124.64, 122.59, 121.68, 120.86, 111.98, 111.125, 109.49, 33.42. CHN Analysis Calcd: C, 61.97; H, 4.09; N, 10.32. Observed: C, 62.16; H, 3.77; N, 10.31.

(B) *mer*- $\text{Ir}(\text{pmb})_3$ .  $^1\text{H}$  NMR (360 MHz,  $\text{CDCl}_3$ ), ppm: 8.16 (d,  $J = 8.7$  Hz, 1H), 8.14 (d,  $J = 8.2$  Hz, 1H), 8.05 (d,  $J = 7.8$  Hz, 1H), 7.85 (d,  $J = 7.5$  Hz, 1H), 7.82 (d,  $J = 7.8$  Hz, 1H), 7.75 (d,  $J = 7.3$  Hz, 1H), 6.46–7.47 (m, 18H), 3.25 (s, 3H), 3.18 (s, 3H), 3.17 (s, 3H).  $^{13}\text{C}$  (90.55 MHz,  $\text{CDCl}_3$ ), ppm: 188.22, 185.95, 184.89, 150.84, 149.64, 149.27, 148.79, 147.86, 147.84, 139.10, 138.93, 136.67, 136.60, 136.22, 132.49, 132.52, 132.48, 124.75, 124.53, 124.34, 122.69, 122.61, 121.86, 121.75, 121.43, 120.61, 120.21, 120.23, 112.35, 111.77, 111.13, 111.09, 111.05, 109.64, 109.56, 109.39, 33.40, 33.39, 33.33, 32.73. CHN Analysis Calcd: C, 61.97; H, 4.09; N, 10.32. Observed: C, 61.88; H, 3.69; N, 10.21.

**X-ray Crystallography.** Diffraction data for *fac*- $\text{Ir}(\text{flz})_3$ , *fac*- $\text{Ir}(\text{pmb})_3$ , and *mer*- $\text{Ir}(\text{pmb})_3$  were collected at  $T = 153(2)$ ,  $143(2)$ , and  $143(2)$  K, respectively. The data sets were collected on a Bruker SMART APEX CCD diffractometer with graphite monochromated Mo  $K\alpha$  radiation ( $\lambda = 0.71073$  Å). The cell parameters for the iridium complexes were obtained from a least-squares refinement of the spots (from 60 collected frames) using the SMART program. Intensity data were processed using the Saint Plus program. All the calculations for the structure determination were carried out using the SHELXTL package (version 5.1).<sup>45</sup> Initial atomic positions were located by Patterson methods using XS, and the structures of the compounds were refined by the least-squares method using SHELX97. Absorption corrections were applied by using SADABS.<sup>46</sup> In most cases, hydrogen positions were input and refined in a riding manner along with the attached carbons. A summary of the refinement details and the resulting factors for the complexes are given in the Supporting Information.

**Electrochemical and Photophysical Characterization.** Cyclic voltammetry and differential pulsed voltammetry were performed using an EG&G potentiostat/galvanostat model 283. Anhydrous DMF was used as the solvent under an inert atmosphere, and 0.1 M tetra-*n*-butylammonium hexafluorophosphate was used as the supporting electrolyte. A glassy carbon rod was used as the working electrode, a platinum wire was used as the counter electrode, and a silver wire was used as a pseudoreference electrode. The redox potentials are based on values measured from differential pulsed voltammetry and are reported relative to either a ferrocenium/ferrocene ( $\text{Cp}_2\text{Fe}^+/\text{Cp}_2\text{Fe}$ ) redox couple or a decamethylferrocenium/decamethylferrocene ( $\text{Me}_5\text{Cp}_2\text{Fe}^+/\text{Me}_5\text{Cp}_2\text{Fe}$ ) redox couple, used as an internal reference.<sup>47</sup>

The UV–visible spectra were recorded on a Hewlett-Packard 4853 diode array spectrophotometer. Steady state emission spectra at room temperature and 77 K were determined using a Photon Technology International QuantaMaster model C-60SE spectrofluorimeter. Phosphorescence lifetime measurements ( $> 2$   $\mu\text{s}$ ) were performed on the same fluorimeter, equipped with a microsecond xenon flashlamp, or on an IBH Fluorocube lifetime instrument by a time correlated single photon counting method using either a 331 or 373 nm LED excitation source. Quantum efficiency (QE) measurements were carried out at room temperature in degassed toluene solutions using the optically dilute method.<sup>48</sup> Solutions of *fac*- $\text{Ir}(\text{ppy})_3$  ( $\Phi = 0.4$ )<sup>6,18a</sup> were used as reference.  $^1\text{H}$  and  $^{13}\text{C}$  NMR spectra were recorded on a Bruker AM 360 MHz instrument, and

(45) Sheldrick, G. M. *SHELXTL*, version 5.1; Bruker Analytical X-ray System, Inc.: Madison, WI, 1997.

(46) Blessing, R. H. *Acta Crystallogr.* **1995**, *A51*, 33.

(47) (a) Gagne, R. R.; Koval, C. A.; Lisensky, G. C. *Inorg. Chem.* **1980**, *19*, 2854. (b) Sawyer, D. T.; Sobkowiak, A.; Roberts, J. L., Jr. *Electrochemistry for Chemists*, 2nd ed.; John Wiley and Sons: New York, 1995; p 467.



### *Phosphorescence from Ir Complexes with Cyclometalated Ligands*

chemical shifts were referenced to residual protiated solvent. Elemental analyses (CHN) were performed at the Microanalysis Laboratory at the University of Illinois, Urbana-Champaign.

**Acknowledgment.** We would like to acknowledge Universal Display Corporation and the Department of Energy for their support of this work.

**Supporting Information Available:** The syntheses of 1-[2-(9,9-dimethylfluorenyl)]pyrazole, 1-phenyl-3-methylimidazolium

iodide, and 1-phenyl-3-methylbenzimidazolium iodide are described. The emission spectrum of flzH at 77 K, cyclic voltammetric traces for *fac*- and *mer*-Ir(pmi)<sub>3</sub> and Ir(pmb)<sub>3</sub>, absorption spectra of *mer*-Ir(pmi)<sub>3</sub> and *mer*-Ir(pmb)<sub>3</sub>, and emission spectra of *fac*- and *mer*-Ir(pmi)<sub>3</sub> at 77 K, as well as crystallographic data for *fac*-Ir(flz)<sub>3</sub> and *fac*- and *mer*-isomers of Ir(pmb)<sub>3</sub> (i.e., tables of bond lengths and angles, crystal data, atomic coordinates, bond distances, bond angles, and anisotropic displacement parameters) are also given. The crystallographic information files (.cif) are also given for each compound.

---

(48) (a) Demas, J. N.; Crosby, G. A. *J. Phys. Chem.* **1978**, *82*, 991. (b) DePriest, J.; Zheng, G. Y.; Goswami, N.; Eichhorn, D. M.; Woods, C.; Rillema, D. P. *Inorg. Chem.* **2000**, *39*, 1955.

IC051296I